SolarPACES 2022, 28th International Conference on Concentrating Solar Power and Chemical Energy Systems
Advanced Materials, Manufacturing, and Components
https://doi.org/10.52825/solarpaces.v1i.674

Published: 15 Mar. 2024

New Coating Paradigm to Boost Performance and Durability of Solar Receivers

Jaione Bengoechea[1][https://orcid.org/0000-0002-1324-8481], Cristina L. Pinto[1][https://orcid.org/0000-0001-6662-3401], Iñaki Cornago[1][https://orcid.org/0000-0001-5882-7287], Alicia Buceta[1][https://orcid.org/0000-0001-8993-4843], Eugenia Zugasti[1][https://orcid.org/0000-0003-2285-5926], Fabienne Sallaberry[1][https://orcid.org/0000-0003-1317-6315], and Marcelino Sánchez[1][https://orcid.org/0000-0001-8690-2539]

[1] CENER (National Renewable Energy Centre of Spain), Solar Energy Technologies and Storage Department, Ciudad de la Innovación 7, 31621 Sarriguren, Spain

Abstract. The development of renewable energy sources is nowadays of enormous importance, not only for the climate change fight but also for the security of the energy supply. The latest geopolitical unfortunate events in Europe have highlighted our energy dependency on foreign fossil fuels. In this context, solar technologies are already playing an essential role in shifting towards neutral carbon economies, ensuring a reliable energy supply. In this regard, dispatchability provided by CSP plants is key to pave the way towards energy transition. It is worth noting that the long-term durability and performance of solar components in arid regions are crucial to increase the reliability and performance of CSP plants while reducing O&M costs. In this work, an innovative approach based on nano-structuring the solar receiver tube glass is presented, which provides improved anti-reflective (AR) and anti-soiling (AS) properties, also showing good durability with respect to abrasion. Spectral transmittance improvement, soiling rate decrease, and durability measurements are presented for nano-structured glasses, comparing with current state of the art glass performance. The achieved experimental results suggest that the new structured glasses would be good candidates for CSP applications.

Keywords: Coating, Solar Receiver Tubes, Optical Property, Durability Tests, Subwavelength Structures

1. Introduction

More than 6 246 MW of solar thermal electric (STE) plants are already installed and operational worldwide and 1 424 MW have been under construction in 2021 [1]. The parabolic trough collector (PTC) is the main technology installed among these electric plants, where the receiver tube is one of its key components. The glass envelope represents the first interface in the transmission of the solar irradiance towards the inner receiver tube before it is absorbed by the heat transfer fluid. As such, the optical properties and the durability of the solar receiver tube are critical in order to guarantee a maximized and reliable energy production of the STE plant.

Nowadays, most manufacturers apply different types of anti-reflective (AR) coatings [2] on glass envelope surfaces, mostly based on porous dielectric materials [3]. However, this strategy is only effective over a limited spectral range and angles of incidence. Moreover, these coatings, commonly deposited by sol-gel [4], are often not as durable as required by the service life. With the aim of solving these challenges, new and more advanced multi-functional surfaces, some of them bioinspired, such as moth-eye or Greta Oto butterfly configurations, are receiving a lot of attention due to their spectrally broadband anti-reflective and omnidirectional

properties [5]-[7]. These structures, characterized by subwavelength sizes, where no light diffraction is produced, act as layers with graded refractive index, ranging from air's (n=1) to glass' (n=1.48) canceling out the reflection at the interface.

In this work, an innovative approach to functionalize the solar receiver tubes, based on nano-structuring the glass envelope surface, is presented. Glass samples have been processed by a simple single-step self-masking RIE (Reactive Ion Etching) process to obtain random subwavelength structures (SWSs), which provide the glass surfaces with spectrally broadband omnidirectional anti-reflective properties, also showing good durability with respect to abrasion. In addition, it is demonstrated that these nano-structures also offer an anti-soiling performance to glass surfaces, a property ambitioned in order to avoid efficiency losses and decrease O&M costs in CSP plants. Spectral transmittance and reflectance improvements, soiling rate decrease and durability measurements are presented in this work for these nano-patterned glasses, comparing with the current state of the art performance, whenever data were available.

2. Methods and materials

For this study, borosilicate glass samples were structured presenting optimum performance nano-structures on their surfaces [8], by means of a simple one-step self-masking RIE process, using fluoride gases mixed with oxygen and argon. Several process parameters, such as gas flow, gas composition ratio, DC bias voltage and chamber pressure have been varied in order to optimize the formation of these nano-structures.

Nano-structured glass surfaces were topologically characterized using a Hitachi S-4700 Scanning Electron Microscope. The spectral transmittance and reflectance of glass samples were measured with a UV/VIS-NIR Perkin Elmer spectrophotometer, model Lambda 1050 with integration sphere, based on IEC Technical Specifications 62862-3-3 [9]. With regard to the anti-soiling property, it was characterized by means of an indoor procedure, specifically developed to compare the adherence of soiling particles to glass samples [8]. In this procedure, glass samples were first weighed using a 4-digit scale and then placed into a hermetic domed chamber, where a total amount 0.5 g of standardized Arizona test Dust A2 was dispersed, settling on all samples equally. Once the deposition finished, samples were weighed again to characterize the homogeneity of the dust deposition procedure along the samples and then, they were vertically placed in a sample holder, which was gently tapped in order to eliminate the non-adhered dust. Finally, samples were weighed a third time to obtain the adhered dust mass. After this deposition phase, the soiling rate was characterized by three parameters: % of dust adhesion using weighing rates, glass surface soiling coverage by means of image processing of samples micrographs, and spectral transmittance measurement.

Finally, the durability of the nano-structured glass AR property was assessed with respect to its resistance to abrasion procedures, which can occur due to cleaning procedures or sand storms in the field. Different abrasion procedures, based on standard IEC 62788-7-3 ED1 [10], were applied to the nano-structured glass with and without the presence of dust as an abrasive medium. The brush block was 40 mm x 25 mm in area and 10 mm in thickness. The brush bristles consisted of polyamide 612 (Nylon), which extended 18 mm from the brush block. Arizona (AZ) Test Dust A2 fine has also been used as an abrasive medium, together with the above described Nylon brush. It is mostly composed of silica (69.0-77.0% of weight) and around 57% of particles are sized between 0.97 μm and 11 μm. Approximately 1500 Pa of pressure was applied to the glass by the brush and the test velocity of about 24 cm/s was defined on the abrasion machine (Figure 1a). Different incremental cycles were applied (100, 200, 300 and 500) onto the same glass sample, where one abrasion cycle consisted of one straightforward and backward movement of the brush. For abrasion with AZ dust, 0.5 g of dust was deposited on the glass sample before the abrasion (Figure 1b), and re-deposited every 100 cycles. Before and after the abrasion procedure, the spectral reflectance from 300 nm to

1600 nm was measured and the damage suffered by the nano-structures was visualized through SEM images.

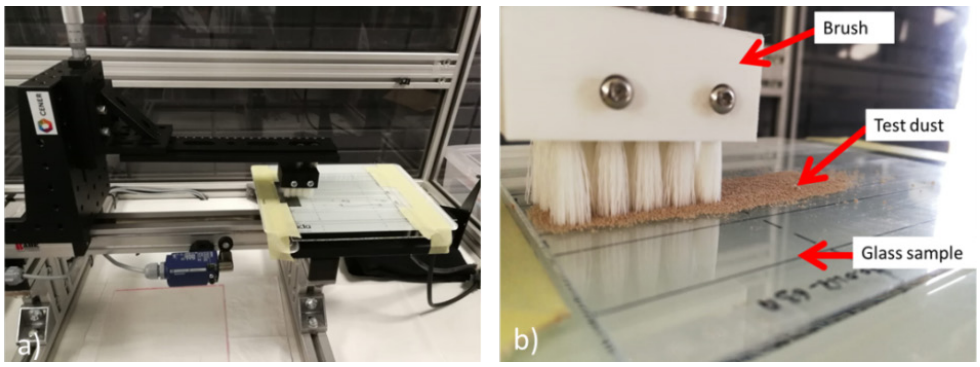

Figure 1. (a) General view of the abrasion test equipment, (b) Images of brush testing procedure with dust.

The glass sample was divided into different sections (guidelines on the non-structured surface) where the incremental test cycles were performed. The marked guidelines in the glass presented 7 cm length where the brush moved at constant velocity and where the optical characterization was performed.

3. Results and discussion

3.1 Optical response

The nano-structures are defined to be subwavelength (SWS) since the distance between adjacent motifs is smaller than the shortest light wavelength and therefore, no light diffraction is produced. These SWSs act as an effective layer with refractive index gradually changing from n = 1 (air) to 1.48 (borosilicate glass) (See Figure 2b), effectively suppressing the reflection in this interface and showing an omnidirectional broadband anti-reflective property. On the contrary, commercial coatings are based on a porous silica layer which acts as a quarter-wave anti-reflective coating with a constant refractive index between air's and glass' (See Figure 2a). These coatings are only effective over a narrow spectral region and also for a limited light angle of incidence due to the abrupt transition between air and glass.

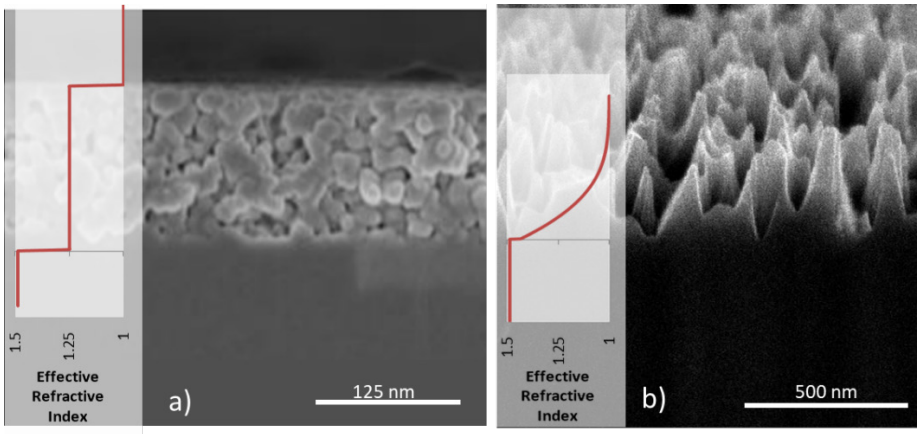

Figure 2. SEM images of (a) a commercial anti-reflective coating (cross-cut view), and (b) the proposed structured glass (tilted view). Together with the SEM images the effective refractive index's spatial variation of each sample is plotted on the left side.

The hemispherical spectral transmittance and reflectance of a structured glass sample have been measured and compared to a flat glass and to a commercial solar receiver glass with AR coating. As it can be appreciated from Figure 3 the flat glass presented a solar transmittance of 92.6 %, but this value can be increased by adding AR coating up to 95.8 %, calculated using a standardized direct solar radiation spectrum between 300 nm and 2500 nm from standard ASTM G123.

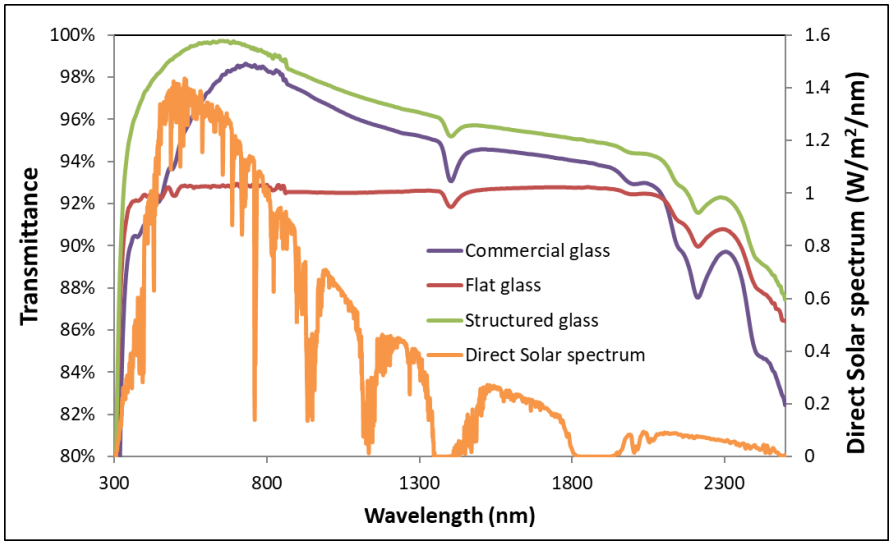

Figure 3. Spectral transmittance of flat glass, structured glass and commercial receiver glass with AR coating. As a reference, the solar spectrum is also plotted.

As illustrated in the figure above, nano-structuring both sides of the glass sample, the transmittance is boosted up to 98.1 %, getting an absolute increase of 2.3% with respect to commercial glass.

In order to complete the optical characterization, the spectral reflectance and its individual components, i. e. specular and diffuse components were obtained too. As it can be seen from Figure 4(a), structured glass shows a broadband anti-reflective property. It presents a solar reflectance of 1.7 %, while the flat glass presented a solar reflectance of 7.5%, which represents an absolute decrease of 5.8%. This improvement in the anti-reflective property can be perfectly appreciated with the bare eye in Figure 4(b), where the reflection from ceiling lights from a flat glass and structured glass is shown.

As was mentioned before, due to the small size of the nano-structures in comparison to the wavelength, the fabricated glass sample does not show any scattering in this spectral range. In order to quantify this behavior, both components of the hemispherical reflected light have been obtained. In this procedure, the hemispherical and diffuse reflectances were measured, while the specular component was obtained from their subtraction. Figure 4(c) plots the specular and diffuse reflectance components averaged from 300 nm to 1600 nm for flat glass and structured glass. As can be understood from this figure, for both flat and structured glass, the specular component dominates.

Finally, with the aim of investigating the reflectance response with respect to the light's angle of incidence, the specular reflectance was measured with Perkin Elmer's URA (Universal Reflectance Accessory), at different angles (8°, 30°, 40°, 50°, and 60°). The results are depicted in Figure 4(d), where structured glass showed an improved directional performance, showing an absolute decrease of 9.4% with respect to the flat glass at 60º of light incident angle.

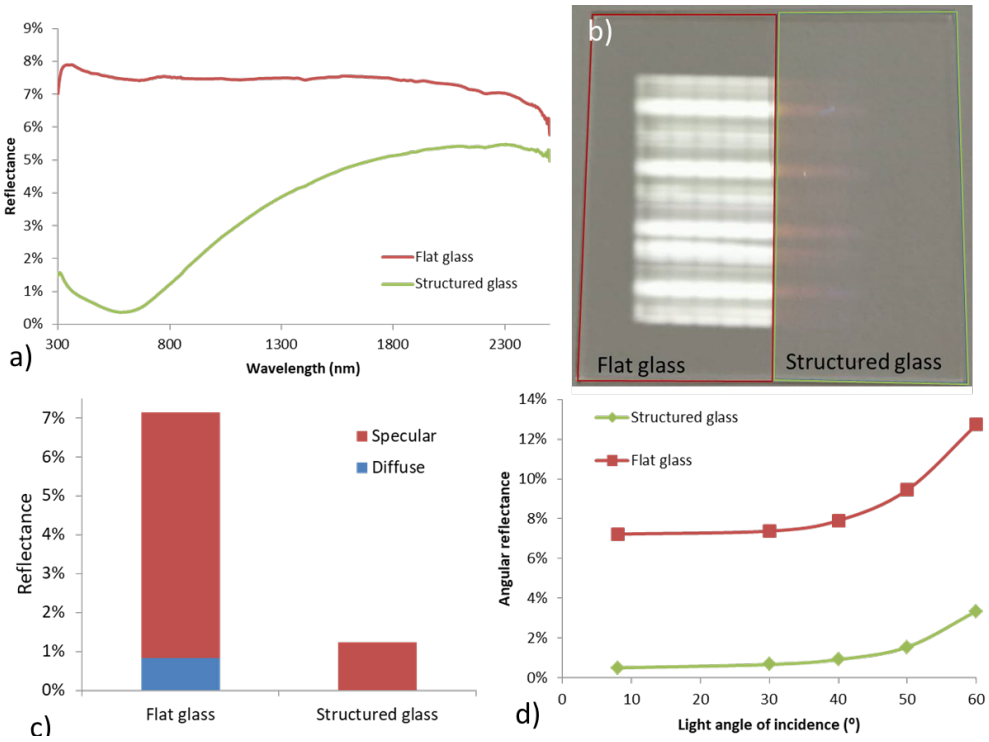

Figure 4. Reflectance measurements.(a) Hemispherical spectral reflectance for flat and structured glass, (b) Photo of a glass sample showing the reflection from a flat and structured glass surface, (c) Reflectance components for flat and structured glass. (d) Specular reflectance for different light incident angles.

3.2 Soiling rate

Soiling refers to the accumulation of dust, soil, organic materials, or other particles on the glass surface. When these dust particles settle on the glass, they cover the surface, reducing the amount of light reaching the solar absorber, and decreasing, therefore, the power output. In fact, in regions where the solar resource is more abundant, i. e. in the Sun Belt, normally the soiling rate is also high [11]-[12]. Even though this soiling rate might depend on the location and environmental conditions, in arid regions like deserts, the transmittance can be reduced by up to 60% in a month. To overcome this issue, anti-soiling property is highly desired.
SWSs increase the mean distance and decrease the contact area between the dust particle and the glass surface, decreasing, therefore, main adhesion forces such as Van der Waals and capillary ones [13]. To characterize the soiling rate, a procedure has been developed which includes a soiling method and three characterization methods including soiling weight, light transmission variation, and surface coverage as it was described in the *Materials and Methods* section. The adhesion percentage is defined in Eq. 1:

$$Adhesion\ (\%) = \frac{Adhered\ dust\ mass}{Deposited\ dust\ mass} \times 100 \qquad (1)$$

This is an important parameter since it provides the relation between the deposited dust and the amount of it which was adhered to sample surfaces. As it can be seen from Figure 5, for flat glass, more than 80%wt of the deposited dust was adhered to its surface. In comparison, for the structured glass, only 37%wt of the deposited dust was adhered to the surface, showing a decrease of more than 55%wt in the soiling ratio.

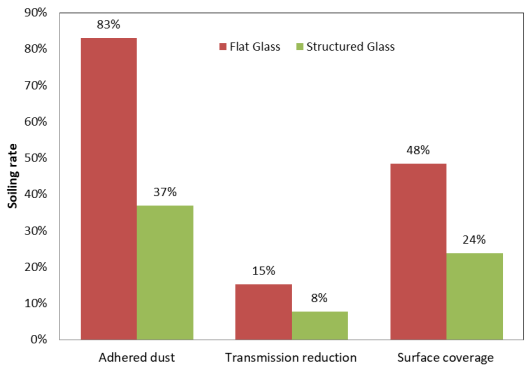

Figure 5. Characterization of flat and structured glass after the soiling procedure.

Regarding the transmittance reduction, the same tendency is kept. For soiled flat glass, the transmittance was reduced by more than 15%, while for structured glass it was only reduced by 7.8%, meaning a decrease of 48% in the soiling rate.
The decrease in transmission is closely related to the surface coverage. In the soiled flat glass, the dust covered 48% of the total surface unlike the structured glass, where the coverage was only of 24%. The soiling ratio decreased slightly more than 50%.
In summary, applying different characterization methods, the soiling rate decreased from 48% to 50% using structured glass.

3.3 Durability

Sand-storms and cleaning procedures can damage or even remove completely the anti-reflective coating from the glasses, decreasing the power generation of the solar thermal plant. In this context, the susceptibility of these nano-structures with respect to abrasion has been investigated in this work. Two abrasion experiments were applied to the structured samples, the first one using a bare Nylon brush as an abrasive medium, and the second one, using Arizona Test Dust A2 together with the Nylon brush. Note that the glass sample was only structured on one side for these tests corresponding to a reflectance of around 4%, which mainly refers to the second interface reflectance.

After the abrasion performed by the Nylon brush, the spectral reflectance was measured obtaining very promising results. Figure 6 a) plots the spectral reflectance of flat glass, structured glass and structured glass after the abrasion produced by the Nylon brush up to 500 cycles. The damage produced by the bristles was negligible, making any notable worsening in the anti-reflective property. Moreover, from SEM images (Figure 6 b), it can be seen that the nano-structures suffered no appreciable damage.

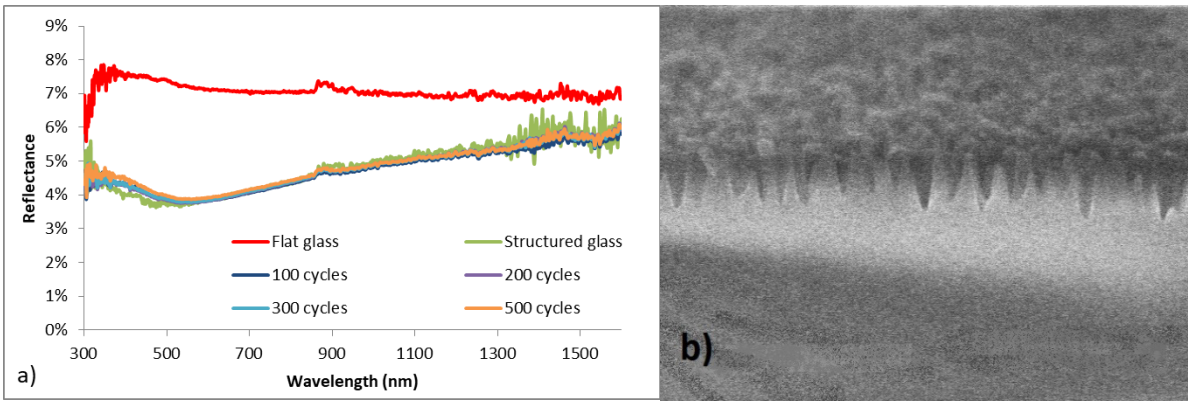

Figure 6. (a) Spectral reflectance of tested glass with Nylon brush, (b) SEM image of the structured glass after 500 cycles of abrasion test with Nylon brush.

Following, the abrasion resistance of SWSs using Arizona Test Dust A2 was investigated. Figure 7a) shows the reflectance of flat glass, structured glass and structured glass after several abrasion cycles. A worsening of 1% absolute on the AR property was observed with respect to the original state for every test carried out. Analyzing the topography of the structured glass (Figure 7b) the abrasion caused by sand and brush can be clearly seen, where most of the nano-structure tips were damaged. Nevertheless, the structures left still presented satisfactory anti-reflective property.

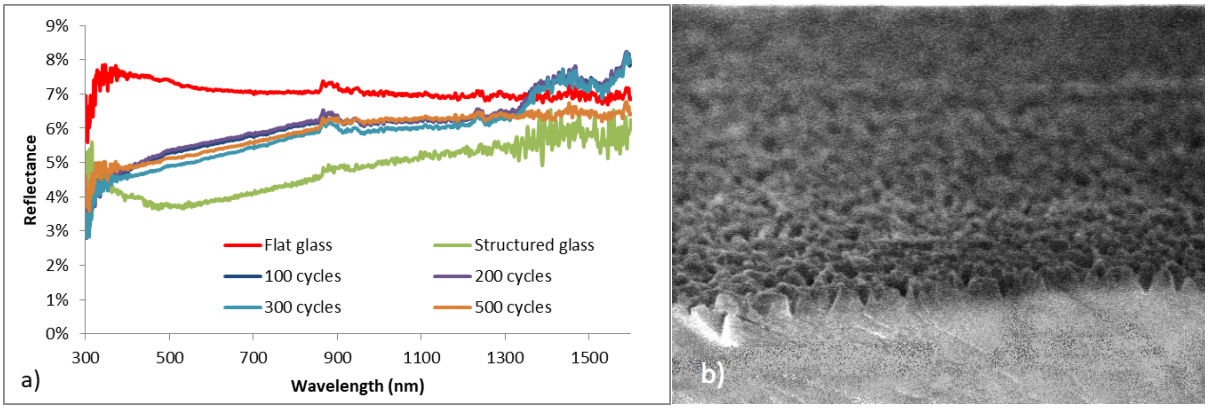

Figure 7. (a) Spectral reflectance of tested glass with AZ dust, (b) SEM image of the structured glass after 500 cycles of abrasion test with dust.

On the other hand, Figure 8 shows the damage produced in two different commercial glasses with ARC after performing the same abrasion test [14, 15]. If we compare our results with the durability of commercial glasses, our structured glass presents a reflectance of 5.6% averaged from 300 nm to 1600 nm. In comparison, commercial glasses, after suffering the same abrasion test, their reflectance increased to almost 7.5% of reflectance, averaged in the same spectral region for 500 abrasion cycles.

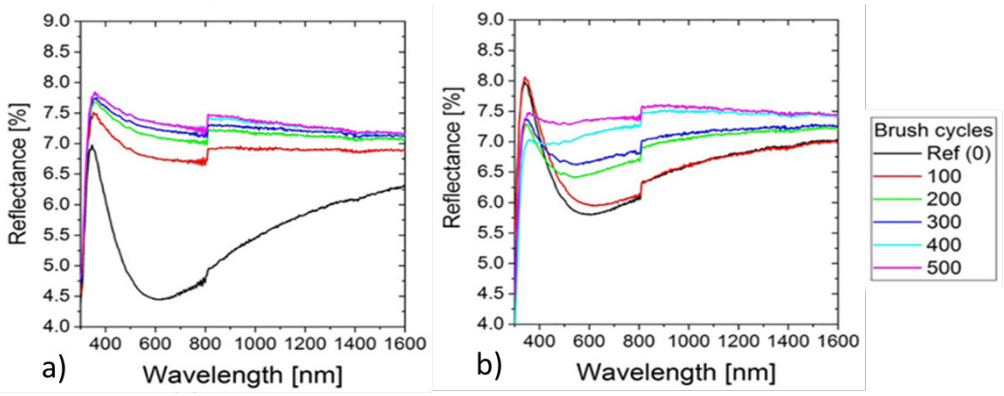

Figure 8. Dust abrasion results of two different commercial PV glasses with ARC [14, 15].

4. Conclusions

A new multifunctional surface paradigm based on a novel approach, i. e. the nano-patterning of glass surface by a simple one-step self-masking RIE process, provides excellent broadband omnidirectional anti-reflectance and anti-soiling properties to solar receiver tubes. More specifically, a solar transmittance increase, with respect to a commercial coating, of approximately 2.3% (absolute) was obtained. Moreover, the anti-soiling behavior has been also quantified, obtaining a reduction in the soiling rate between 48% - 50%, with respect to a flat glass. The durability of these structures has also been investigated, applying the main guidelines stated in standard IEC-62788-7-3 [10], obtaining very promising results.

Data availability statement

The data that support the findings of this study are available on request from the corresponding author, Jaione Bengoechea (jbapezteguia@cener.com). The data are not publicly available since their use could compromise CENER's interest on their exploitation.

Author contributions

Jaione Bengoechea: Conceptualization, Methodology, Writing- review & editing, Project administration. **Cristina L. Pinto:** Methodology, Investigation, Data curation, Formal Analysis Writing – original draft. **Iñaki Cornago**: Conceptualization, Methodology, Investigation, Writing – review & editing, Supervision. **Alicia Buceta**: Investigation. **Eugenia Zugasti**: Conceptualization, Investigation. **Fabienne Sallaberry**: Writing – review & editing. **Marcelino Sanchez:** Supervision, Project administration.

Competing interests

The authors declare no competing interests.

Acknowledgement

Cristina Pinto gratefully acknowledges the Department of University, Innovation and Digital Transformation of the Government of Navarra for the grant for hiring doctoral students and doctoral students by companies, research centers, and technology centers: Industrial Doctorates 2020, with file number 0011-1408-2020-000003, received to carry out this study.

References

1. SolarPACES web page https://www.solarpaces.org/wp-content/uploads/installed_capacity_sept2021.jpg
2. A. Grosjean, A. Soum-Glaude, P. Neveu and L. Thomas, "Comprehensive simulation and optimization of porous SiO2 antireflective coating to improve glass solar transmittance for solar energy applications", Solar Energy Materials and Solar Cells, vol. 182, no. 1, pp. 166-177, August, 2018, doi: https://doi.org/10.1016/j.solmat.2018.03.040
3. G. San Vicente, R. Bayón, N. Germán, and A. Morales, "Surface modification of porous antireflective coatings for solar glass covers", Sol. Energy, vol. 85, no. 4, pp. 676–680, Apr. 2011, doi: https://doi.org/10.1016/J.SOLENER.2010.06.009.
4. G. San Vicente, R. Bayón, N. Germán and A. Morales, "Long-term durability of sol–gel porous coatings for solar glass covers", Thin Solid Films, vol. 517, no. 10, pp. 3157-3160, March 2009, doi: https://doi.org/10.1016/j.tsf.2008.11.079.
5. R. H. Siddique, G. Gomard, and H. Hölscher, "The role of random nanostructures for the omnidirectional anti-reflection properties of the glasswing butterfly," Nat. Commun., vol. 6, pp. 1–8, 2015, doi: https://doi.org/ 10.1038/ncomms7909.
6. B. M. Phillips and P. Jiang, "Biomimetic Antireflection Surfaces," in Engineered Biomimicry, Gainesville: Elsevier Inc., 2013, pp. 305–331, doi: https://doi.org/10.1016/B978-0-12-415995-2.00012-X
7. S. Chattopadhyay, Y. F. Huang, Y. J. Jen, A. Ganguly, K. H. Chen, and L. C. Chen, "Anti-reflecting and photonic nanostructures," Mater. Sci. Eng. R Reports, vol. 69, no. 1–3, pp. 1–35, 2010, doi: https://doi.org/ 10.1016/j.mser.2010.04.001.
8. C. L. Pinto, I. Cornago, A. Buceta, E. Zugasti, and J. Bengoechea, "Random subwavelength structures on glass to improve photovoltaic module performance," Sol. Energy Mater. Sol. Cells, vol. 246, no. August, p. 111935, 2022, doi: https://doi.org/10.1016/j.solmat.2022.111935

9. F. Sallaberry, A. García de Jalón, J. García Barberena, and I. David Bernad, “Standardized testing of receiver tubes and solar mirrors of parabolic trough solar thermal power plants”, AIP Conference Proceedings vol. 2126, 120019, 2019, doi: https://doi.org/10.1063/1.5117637.
10. Standard IEC-62788-7-3:2022, Measurement procedures for materials used in photovoltaic modules - Part 7-3: Accelerated stress tests - Methods of abrasion of PV module external surfaces, 2022.
11. H. Qasem, “Effect of accumulated dust on the performance of photovoltaic modules,” Loughborough University, 2013
12. T. Sarver, A. Al-Qaraghuli, and L. L. Kazmerski, “A comprehensive review of the impact of dust on the use of solar energy: History, investigations, results, literature, and mitigation approaches,” Renew. Sustain. Energy Rev., vol. 22, pp. 698–733, 2013, doi: https://doi.org/10.1016/j.rser.2012.12.065.
13. S. You and M. P. Wan, “Mathematical models for the van der Waals force and capillary force between a rough particle and surface,” Langmuir, vol. 29, no. 29, pp. 9104–9117, 2013, doi: https://doi.org/10.1021/la401516m.
14. M. Z. Khan *et al.*, “Resilience of industrial PV module glass coatings to cleaning processes,” *J. Renew. Sustain. Energy*, vol. 12, no. 5, 2020, doi: 10.1063/5.0024452
15. K. Ilse, P.-T. Miclea, V. Naumann, and C. Hagendorf, “Cleaning resistance of glass coatings.” Fraunhofer, 2018, [Online]. Available: https://www.csp.fraunhofer.de/content/dam/imws/csp/de/documents/Diagnostik/Test%20report%20V403_2018%20-%20Cleaning%20resistance%20of%20glass%20coatings.pdf